Vapor Pressures in the Al(l) + Al_2O_3(s) System: Reconsidering Al_2O_3(s) Condensation

Evan Copland

Case Western Reserve University / NASA Glenn Research Center, Department of Materials Science and Engineering, Cleveland, Ohio, USA

Abstract

The vaporization behavior of the Al-O system has been studied on numerous occasions but significant uncertainties remain. The origin of this uncertainty must be understood before Al-O vaporization behavior can be accurately determined. The condensation of Al_2O_3 and clogging of the effusion orifice is a difficult problem for the Knudsen effusion technique that influences the measured vaporization behavior but has only received limited attention. This study reconsiders this behavior in detail. A new theory for Al_2O_3 condensation is proposed together with procedures that will improve the measured thermodynamic properties of Al-O vaporization.

Keywords: Al(g) and Al_2O(g) vaporization; Al_2O_3(s) condensation; improving thermodynamic measurements; multiple effusion cell mass spectrometry.

1. Introduction

The vaporization behavior of the Al-O system has been investigated in numerous studies since the early 1950's. These studies used the effusion-method, in its various forms, to sample the vapor phase in equilibrium with Al(l) + Al_2O_3(s) [1-4] and Al_2O_2(s) [1, 5, 6] in a range of container materials. In spite of this level of investigation, some vapor species and the thermodynamics of vaporization are still not fully understood. Recently there has been renewed interest in Al-O vaporization [7-9]. Improving the thermodynamic data of the Al-O system will allow more accurate measurements of the alloy + oxide equilibrium in the Ni-Al, Ti-Al and Fe-Al systems [10]. This information will improve our understanding

of high-temperature oxidation behavior of these systems which rely on the formation of a protective Al_2O_3(s) surface-layer by reaction with oxygen containing atmospheres. To do this, however, a more fundamental investigations of Al(l) + Al_2O_3(s) vaporization is needed.

A range of vapor species have been identified in the Al-O system: Al(g), Al_2O(g), Al_2(g), AlO(g), AlO_2(g), Al_2O_2(g), Al_2O_3(g), O(g) and O_2(g) [1-6]. Questions remain about the existence of AlO_2(g) [8]. The composition of the vapor depends on the oxygen partial pressure. At low $p(O_2)$, when Al(s,l) and α-Al_2O_3(s,l) are stable, Al(g) and Al_2O(g) dominate while at higher $p(O_2)$, when α-Al_2O_3(s,l) is stable, O(g), Al(g) and AlO(g) typically dominate. To quantify the uncertainty in Al-O vaporization reaction enthalpies measured by this author are compared to the accepted values [11-13] in table 1. The details of these new measurements will be discussed in a subsequent paper. While these results differ significantly, it is not constructive to propose changing generally accepted thermodynamic properties without first investigating possible reasons for the discrepancies and suggesting improved experimental procedures. Accordingly, two likely sources of error are: 1) reaction between Al(l) and the effusion-cell material, and 2) clogging the effusion orifice at high temperatures with the condensation of Al_2O_3(s,l).

TABLE 1

Comparison of Reaction Enthalpies in Al-O system, $\Delta_R H°(298.15K)$

Reaction	Measured[14] (kJ/mol)	IVTAN[11] (kJ/mol)	JANAF[12] (kJ/mol)
Al(s,l) = Al(g)	[redacted]	330.0±3.0	329.7±4.2
4/3Al(s,l) + 1/3Al_2O_3(s) = Al_2O(g)	[redacted]	409.0±56	413.4±50
4/3Al(g) + 1/3Al_2O_3(s) = Al_2O(g)	[redacted]	-30.0±4.3	-26.2±3.0
2Al(g) + O(g) = Al_2O(g)	[redacted]	-1057.0±20	-1053.7±150

[redacted]

Identifying a suitable container material is important for all thermodynamic measurements and a range of materials (*i.e.*, BeO, TaC, ZrO_2, Al_2O_3, Mo and W) have been used in Al-O vaporization studies. Brewer and Searcy used BeO and TaC effusion-cells but Al(l) reacted with both materials [1]. Porter *et al.*, used a ZrO_2-liner in a Ta effusion-cell without reporting any significant reaction [2]. Motzfeldt *et al.* successfully used a Al_2O_3 effusion-cell [3, 4]. Mo and W have been used extensively to study the vaporization of Al_2O_3 but both are unsuitable for Al(l). According to the condensed phase diagrams, Al-O

[15], Al-Zr-O [16], and Al_2O_3-ZrO_2-Y_2O_3 [17, 18]. Al_2O_3 is best suited for studying the vaporization of Al(l) + Al_2O_3(s) as ZrO_2-based containers will react with Al(l). The affect of a ZrO_2-based effusion-cell was recently considered by directly comparing the vapor pressures of Al(g) and Al_2O(g) in equilibrium with Al(l) in a ZrO_2 effusion-cell and Al(l) in a Al_2O_3 effusion-cell [7]. These results showed Al(l) remained pure and a Al_2O_3-layer formed on the inner surface of the ZrO_2 effusion-cell, effectively transforming it into an Al_2O_3 effusion-cell and making it thermodynamically identical to Al(l) + Al_2O_3(s). While interesting, this result showed that a ZrO_2 effusion-cell does not change the measured vaporization behavior in the Al-O system. This leaves the difficult problem of Al_2O_3 condensation.

Al_2O_3 condensation has been observed by this author while measuring the vaporization behavior of Al(l) + Al_2O_3(s) and γ-TiAl(s) + Y_2O_3(s) and was previously observed for Al(l) + Al_2O_3(s) by Motzfeldt *et al.* [3, 4] and for Al_2O_3(l) by Drowart *et al.* [5]. It occurs on the outer edge of the orifice, is more pronounced for small diameter orifices (less then about 1.0mm) and is usually only noticed at temperatures above about 1500 K. Condensation of Al_2O_3 will influence the measured vaporization behavior by changing the shape of the effusion orifice and therefore the rate of effusion independent of the partial pressures inside the effusion-cell. This behavior appears to be typical for systems with high aluminum activity, and it is surprising that it has only received limited discussion. Motzfeldt *et al.* appears to be the only research to consider this problem and their experiments and discussion are reviewed.

1.2 Motzfeldt's investigation of Al_2O_3-condensation

This problem was considered on two occasions while studying the vaporization of Al(l) + Al_2O_3(s) in an Al_2O_3(s) effusion-cell by a classical effusion method with continuous thermogravimetic monitoring of the rate of mass loss. The first study was conducted at 1585 and 1623 K in a tube furnace with a graphite heating element and with effusion orifices ranging from 0.8 to 8.0 mm in diameter [3]. The second study was at 1556 K in a furnace with a molybdenum heating element and with effusion orifices ranging from 0.6 to 2.9 mm in diameter [4]. In all experiments, pure Al(s) with excess Al_2O_3(s) was loaded into Al_2O_3 effusion-cells. From previous mass spectrometric studies [2, 5, 6] Al(g) and Al_2O(g) were assumed to be the dominant vapor species and it was explicitly assumed that there was no mass loss due to vaporization of

the outer surface of the Al_2O_3 effusion-cell and implicitly assumed that the effusion cell did not gain mass by reaction with the furnace environment. Following these assumptions the measured mass loss for the system (sample + effusion cell) was due solely to the effusion of Al(g) and Al_2O(g) at partial pressures p(Al) and $p(Al_2O)$, according to the vaporization reactions Eq. (1) and Eq. (2). This occurs at a rate (mol·s^{-1}) for each species according to the Hertz-Knudsen relation Eq. (3):

$$Al(l) = Al(g) \tag{1}$$

$$4Al(l) + Al_2O_3(s) = 3Al_2O(g) \tag{2}$$

$$dn_i/dt = p(i)A_oW_o/(2\pi RM_iT)^{1/2} \tag{3}$$

where n_i is number of moles, p(i) is the partial pressure, A_o is the area of the orifice, W_o is the Clausing factor or the orifice, R is the gas constant, M_i is the molar mass and T is the absolute temperature. The total mass loss, Δq, is due to consumption of Al(l) and Al_2O_3(s) in the cell ($\Delta q = \Delta n_{Al} \cdot M_{Al} + \Delta n_{Al_2O_3} \cdot M_{Al_2O_3}$). The moles of Al(l) consumed, Δn_{Al}, were determined by measuring how much Al(s) remained while Al_2O_3(s) consumption, $\Delta n_{Al_2O_3}$, was determined by the difference between the total mass loss and measured Al(l) consumption $\left(\Delta q - \Delta n_{Al} \cdot M_{Al}\right)/M_{Al_2O_3}$. For each mole of Al_2O_3 four moles of Al(l) were consumed due to the effusion of three 3 moles of Al_2O(g) according to Eq. (2). The excess moles of Al(l) lost were attributed to reaction (1) and the effusion of Al(g). In this way the number of moles Al(g), n_{Al}, and Al_2O(g), n_{Al_2O}, lost by effusion during the experiment were determined and used to calculate p(Al) and $p(Al_2O)$ according to Eq. (3). The total rate of mass loss (g·s^{-1}) is the sum of the effusion of Al(g) and Al_2O(g), Eq. (4), and is constant at a fixed temperature.

$$dq/dt = A_oW_o/(2\pi RT)^{1/2}\left(p(Al)(M_{Al})^{1/2} + p(Al_2O)(M_{Al_2O})^{1/2}\right) \tag{4}$$

In both studies, however, the rate of mass loss was not constant but decreased with time. This was more pronounced for smaller effusion orifices and occurred at a faster rate in the first study. This behavior

was attributed to Al_2O_3 condensation on the outer edge of the orifice that reduced the orifice area, A_o, and changed the Clausing factor, W_o, during the course of each experiment. A temperature gradient was ruled out because no condensation was observed inside of the cell lid and a significant effort was made to ensure an isothermal condition. No explanation was proposed for Al_2O_3 condensation in the first study but it was noted that the ratio of the partial pressures of the species, F, was related to the effusion orifice area. It was suggested that this could be due $Al_2O(g)$ reacting with the graphite heating element and the formation of excess Al(g) outside the effusion-cell, according to reaction (6). The excess Al(g) could then react with the outside of the effusion-cell resulting in an increased loss of $Al_2O_3(s)$, according to reaction (7). To test this a molybdenum heating element was used in the second study. Data was obtained by extrapolating the measured rate of mass loss to the start of the experiment when the shape of the orifice was known.

$$F = p(Al_2O)/p(Al) = n_{Al_2O}\left(M_{Al_2O}\right)^{1/2}/n_{Al}\left(M_{Al}\right)^{1/2} \quad (5)$$

$$Al_2O(g) + C(s) = 2Al(g) + CO(g) \quad (6)$$

$$4Al(g) + Al_2O_3(s) = 3Al_2O(g) \quad (7)$$

The second study [4] used the same analysis procedure and similar behavior was observed but the rate of orifice clogging and the increase in F with orifice area was less pronounced. The variation in F with orifice area was accepted as real but unrelated to the heating element material. A complex calculation procedure was developed to consider an average effective orifice area, A_{ave}, to correct for the decreasing orifice area with time. In addition, the concept of "hindered" vaporization for Al(g), $\alpha_{vap}(Al) < 1$, from $Al_2O_3(s)$ was introduce to explain the apparent decrease in measured $p(Al)$ with increasing orifice area (while $p(Al_2O)$ was assumed to be independent of orifice area). This was used, with reaction (7), to explain the "unavoidable" Al_2O_3 condensation. The reduced $p(Al)$ in the effusion orifice acts to shift the equilibrium in reaction (7) to the left, resulting in condensation of $Al_2O_3(s)$.

These studies clearly involved a large amount of detailed experimental work, however, there are several obvious problems in the interpretation of these results that need to be identified. The first problem is the mass balance analysis used to determine the number of moles of Al(l) and $Al_2O_3(s)$ lost from the

system. The analysis technique did not allow the vaporization processes inside the cell and effusion from the cell to be treated separately from the condensation of Al_2O_3 on the outside of the cell. A portion of material transported from inside the effusion-cell did not leave the system but condensed as Al_2O_3 on the outside of the cell. Therefore the measured mass loss is less then the actual amount of Al(l) and Al_2O_3(s) removed from inside of the cell. In this situation the analysis procedure underestimates the moles of Al_2O_3(s) consumption which results in both a low $p(Al_2O)$ and high $p(Al)$. As the amount of Al_2O_3 condensation increases relative to the orifice area (as the orifice area decreases) F must decrease. Thus, the behavior observed for F can be explained without considering "hindered" vaporization of Al(g) and the best results should be obtained with the largest orifices where the relative amount of orifice clogging is the smallest. While a reduced vaporization coefficient for Al(g) from Al_2O_3(s) is possible, its effect would be difficult to observe with a Al(l) + Al_2O_3(s) mixture as Al(g) vaporization from Al(l) would dominate. As a general rule the more complex vapor species is more likely to experience hindered vaporization, that is $\alpha_{vap}(Al_2O) < \alpha_{vap}(Al)$ [19]. Further, if a reduced $\alpha_{vap}(Al)$ was the reason for Al_2O_3 condensation then as the effusion orifice clogs $p(Al)$ would increase as it is more accurately sampled. This would shift equilibrium of reaction (7) to the right and limit further condensation, against the observation that Al_2O_3 condensation is more pronounced for smaller orifices. These problems raise uncertainty about Motzfeldt's theory. An obvious test of this theory is to measure F with time as the effusion orifice clogs due to Al_2O_3 condensation. This is a relatively simple experiment for effusion cell vapor source coupled to a mass spectrometer, *KEMS*. This experiment is described and the results considered.

2. Experimental

2.1. Materials

In this study about 0.5 g of Al(s) (99.9999 wt% purity) were loaded into an Al_2O_3 effusion-cell (99.99 wt% purity) shown schematically in figure 1. Prior to use the effusion cell was cleaned by baking at about 1800 K for 10 hours under vacuum (~10^{-3} Pa). In addition, a sample of Au (99.9999 wt% purity) was

placed in a graphite-liner inside a second Al_2O_3 effusion-cell, in the isothermal zone of the furnace, and was used to check for temperature and instrument sensitivity during the experiment.

2.2. Apparatus and Experimental Procedure

These measurements were made with a Nuclide/MAAS/PATCO 12-90-HT single focus magnetic sector mass spectrometer coupled to a multiple effusion-cell vapor source. The relative partial pressures of Au(g), Al(g) and Al_2O(g) were determined indirectly by sampling their flux in a molecular beam (selected from the distribution of effusing molecules) by electron impact resulting in Au^+, Al^+ and Al_2O^+ ions and the formation of a representative ion beam that was sorted according to mass-to-charge ratio by common mass spectrometric techniques. An electron energy of about 25eV was used and there was no evidence of Al_2O(g) fragmentation. The partial pressures, p(i), in the effusion-cell is related to the measured intensity of each ion, I_i, and absolute temperature, T, by Eq. (8) [20].

$$p(\mathrm{i}) = I_i T / S_i \tag{8}$$

S_i is the instrument sensitivity factor and is a complex function of the: intersection of the molecular and electron beams, ion extraction efficiency, ionization cross-section, transmission probability of the mass analyzer, detector efficiency and isotopic abundance. Absolute pressure measurements are difficult, as a result S_i is typically assumed constant and relative partial pressures are considered (*i.e.*, $p(\mathrm{i}) \propto I_i T$). In this way F was monitored directly by measuring the ion intensity ratio of Al_2O^+ and Al^+ with time, Eq. (9).

$$F \propto I_{Al_2O} / I_{Al} \tag{9}$$

The effusion cells were maintained at 1550±3.0 K over 8 hours during which time a consistent portion of the effusing molecules from each cell were samples at 45 minute intervals while the orifice of the cell containing Al(l) partial clogged with the condensation of Al_2O_3. From Eq. (3) the rate and the distribution

of Al(g) and Al_2O(g) effusing form the orifice will change with time as the orifice closes. This will change their flux distribution in the molecular beam and therefore the rate of ion production independent of $p(Al_2O)$ and $p(Al)$ in the effusion-cell, however, as both species are sampled with the same orifice the effect is identical.

The successful application of a multiple effusion-cell vapor sources requires that vapor pressure can be consistently sampled independent of the effusion-cell. This condition is obtained with the inclusion of two fixed apertures (field and source) between the effusion cell and ion source and accurate alignment of the orifice [14, 21-23]. The fixed apertures define an ionization volume independent of vapor source and the alignment of the orifice is monitored visually with a video camera mounted above the ion source that sights through the fixed apertures [14]. The temperature was measured with a pyrometer (Mikron M190V-TS) sighting a blackbody source (2.5 mm in diameter and 13.5 mm long) machined into the bottom of the effusion-cell and Mo-cell holder.

3. Results

Al_2O_3 condensed and clogged the effusion orifice over 8 hours at 1550±3 K and was observed visually and as a drop in the measured ion intensities of Al^+ and Al_2O^+ with time. In addition to growth on the outer edge of the effusion orifice, Al_2O_3 "needles or whiskers" also grew from other surfaces in the furnace in a direct line from the effusion orifice. These areas are identified in the cross section of the furnace shown in figure 2. The extent of clogging after 8 hours is shown in the SEM image of the outside of the orifice, shown in figure 3. The Al_2O_3 crystals have grown out of the plane of the orifice (30~60° to the normal) and range widely in thickness.

The temperature and instrument sensitivity were monitored during the experiment and the ion intensity of Au^+ from the effusion cell containing pure Au(l) is shown in figure 4. Over 8 hours the furnace temperature slowly increased from 1547 K to 1552 K while I_{Au} remained consistent (5342±180 K). This indicates a small decrease in instrument sensitivity but this is not expected affect any other results. The variation in the measured ion intensities of Al^+, Al_2O^+ and F, as the effusion orifice closed, are shown in figure 5. During an initial period, ~2 hours, the measured ion intensities of Al^+ and Al_2O^+ were constant.

This is expected to be due to a "restricted collimation" condition imposed by the fixed apertures that define the source area, A_s, of the molecular beam that is smaller then the cross section of the effusion orifice, A_o [22, 23]. As a result the flux distribution of Al(g) and Al_2O(g) in the molecular beam remained relatively unchanged until the growth of Al_2O_3 condensation encroaches into the source area, A_s. Following this period, the measured ion intensities of Al^+ and Al_2O^+ dropped about 41% over 6 hours as the Al_2O_3 crystals continued to grow. F remained consistent with only a small increase with time consistent with the measured temperature drift and the reaction enthalpies reported in table 1.

4. Discussion

Observing that the measured ratio of $p(Al_2O)/p(Al)$ remained consistent as the orifice closed provides direct evidence that hindered vaporization of Al(g) from Al_2O_3(s) inside the effusion cell is not the reason for the condensation of Al_2O_3. The condensation of Al_2O_3 can be easily understood when it is recognized that inside the effusion cell Al(g) and Al_2O(g) are in equilibrium with Al(l) + Al_2O_3(s) and this equilibrium also defines a partial pressure of O_2(g) in the order of 10^{-42} to 10^{-20} Pa (and O(g) 10^{-24} to 10^{-12} Pa) over the temperature range 1000 K to 1600 K. The environment outside the effusion-cell in a furnace containing Ta can contain O_2(g) pressures up to 10^{-29} to 10^{-12} Pa [11]. This is many orders of magnitude higher then that in equilibrium with Al(l) + Al_2O_3(s) which allows the Al_2O_3 effusion cell remain stable. Therefore as Al and Al_2O molecules leave the effusion cell they enter an environment with a greatly increased oxygen activity which results in a large driving force for Al_2O_3(s) formation. At reduced pressures (~10^{-4} Pa) a heterogeneous reaction between Al(g), Al_2O(g) and oxygen containing species (O_2(g), O(g), H_2O(g), Al_2O(g),...) on a surface is more probable than homogeneous precipitation of Al_2O_3(s) in the vapor phase. Therefore it is proposed that Al_2O_3 condensation occurs by beterogeneous growth by the reaction of impinging fluxes of Al(g) or Al_2O(g) molecules with oxygen containing species on a Al_2O_3-surface according to either:

$$2Al(g) + 3O(ads) = Al_2O_3(s) \quad (10a)$$

$$Al_2O(g) + 2O(ads) = Al_2O_3(s) \quad (10b)$$

It is unclear which reaction dominates the growth rate of $Al_2O_3(s)$. This would be difficult to determine and is outside of the scope of this investigation. In general terms, the growth kinetics depend on: the flux of $Al_2O(g)$, Al(g) and oxygen containing species; their condensation coefficients; the adsorption process; and the crystallographic orientation of the Al_2O_3 relative to the vapor flux [24]. According to this theory, as the temperature is increased the growth rate of condensed Al_2O_3 will increase in proportion to $p(Al_2O)$ and $p(Al)$, provided there is an adequate supply of oxygen. Therefore the higher Al_2O_3 growth rate observed in Motzfeldt's first study can probably be attributed to the higher temperatures (1585 K and 1623 K as opposed to 1556 K) rather then the different heating element materials (graphite and Mo).

Even though Al(g) and $Al_2O(g)$ are reacting to form $Al_2O_3(s)$ this will not change the measured $p(Al_2O)/p(Al)$ ratio because only molecules that don't reacted to form $Al_2O_3(s)$ reach the ion-source. The molecular beam will therefore retain the equilibrium $p(Al_2O)/p(Al)$ ratio defined by $Al(l) + Al_2O_3(s)$ inside the effusion-cell. Some vaporization will occur from the condensed $Al_2O_3(s)$ within the source area, A_s, of the molecular beam, however, the increased oxygen activity of the furnace environment mean $Al_2O(g)$ and Al(g) no longer dominant. Therefore the contribution of $Al_2O(g)$ and Al(g) vaporizing from the condensed $Al_2O_3(s)$ to the molecular beam would be insignificant compared to that coming from within the effusion cell, until the point when the orifice is almost completely closed. Therefore clogging of the orifice by Al_2O_3 condensation can be thought of solely as changing the effective orifice-area and the associated change in the distribution of effusing molecules. As orifice clogging is more pronounced at high temperatures, pressure measurements made at higher temperatures are more effected, reducing the measured enthalpies of vaporization of both Al(g) and $Al_2O(g)$, as seen in table 1. Improving thermodynamic measurements in the Al-O system requires that the affect of Al_2O_3 condensation is reduced to a minimum.

4.1 Suggestions for improved thermodynamic measurements

According to this theory, the condensation of $Al_2O_3(s)$ must occur at all temperatures but it only occurs at an observable rate when $p(Al)$ and $p(Al_2O)$ are high enough to provide a significant molecular flux to the

Al_2O_3-surface for a given $p(O_2)$. Therefore more accurate thermodynamic data in the Al-O system can be obtained by: 1) limiting measurements to temperatures below about 1450 K with the highest temperature measurement taken first, or 2) reducing the $p(O_2)$ inside the furnace to levels that approach those in equilibrium with Al(l) + Al_2O_3(s). The first option may not initially appear satisfactory, however, the upper pressure-limit of the Knudsen-effusion technique (~1 Pa), imposed by molecular flow conditions, already limits the temperature to about 1600 K. Reducing $p(O_2)$ to these levels requires the introduction of "oxygen-getters" (in the form of Ti, Zr or Hf sheets) inside the multiple effusion cell furnace and the vacuum chamber. These have been added to the furnace as shown in figure 2 but additional heated sheets are probably required outside the furnace, particularly around the field aperture and also inside the ion source chamber. Obviously there is a limit to reducing $p(O_2)$ as the Al_2O_3 effusion-cell must remain stable. It is also important to notice that this behavior is likely to occur in other metal-oxygen systems that contain very stable oxides, for example Y-O, Zr-O, Ti-O.

While this investigation has focused on the heterogeneous growth of Al_2O_3 there is no reason to assume that corresponding homogenous reactions are not also occurring within the molecular beam between the orifice and the ion source. Homogenous reactions between Al(g) and Al_2O(g) in the molecular beam and O_2(g) or O(g) in the vacuum chamber could result in the formation of AlO, AlO_2, Al_2O_2 and Al_2O_3 molecules unrelated to the sample being studied within the effusion cell. Reducing $p(O_2)$ inside the vacuum chamber will help to limit these reactions and further improve thermodynamic measurements in the Al-O system.

5. Conclusions

In an effort to better determine the thermodynamic properties of vapor species in the Al-O system the problem of Al_2O_3 condensation and orifice clogging was reconsidered. Motzfeldt's theory for Al_2O_3 condensation was reviewed and serious questions were raised about its validity. This theory was basis on the apparent increase in $p(Al_2O)/p(Al)$ with effusion orifice area and this was attributed to "hindered" vaporization of Al(g) from Al_2O_3(s). This study tested this assumption by monitoring $p(Al_2O)/p(Al)$ over 8 hours at 1550±3 K while the effusion orifice clogged due with the growth of Al_2O_3 crystals. A consistent

$p(Al_2O)/p(Al)$ ratio was observed during this period while the measured partial pressures of $Al_2O(g)$ and Al(g) both dropped about 41%. This disagrees with the previous explanation for Al_2O_3 condensation. A much simpler explanation was proposed based on the large difference in $p(O_2)$ between the inside of the effusion cell (defined by the Al(l) + Al_2O_3(s) equilibrium) and the furnace environment. As the Al and Al_2O molecules leave the effusion-cell they enter an environment with a greatly increased $p(O_2)$ and Al_2O_3 condensation occurs by heterogeneous growth by the reaction of impinging Al(g) or Al_2O(g) molecules with absorbed O on a Al_2O_3-surface. According to this theory Al_2O_3 condensation occurs at all temperatures while studying Al(l) + Al_2O_3(s) but it only occurs at an observable rate at temperatures above 1500 K when the fluxes of Al(g) and Al_2O(g) are high. To obtain more accurate thermodynamic data in the Al-O system it was proposed to either: 1) limit measurements to below about 1450K with the highest temperature measurement taken first, or 2) reduce the $p(O_2)$ inside the furnace to levels that approach the dissociation pressure in equilibrium with Al(l) + Al_2O_3(s). A combination of both is currently being tried.

Acknowledgements

The help of Christian Chatillon and Nathan Jacobson in preparing this manuscript and providing insightful discussion is gratefully acknowledged. The funding for this work came from NASA Glenn Research Centre's Low Emission Alternative Power Project.

References

[1] L. Brewer and A. Searcy, J. Am. Chem. Soc., 73 (1951), 5308-5314.
[2] R. Porter, P. Schissel and M. Inghram, J. Chem. Phys., 23 (1955), 339-342.
[3] O. Herstad and K. Motzfeldt, Rev. Hautes Temper. et Refract., 3 (1966), 291-300.
[4] D. B. Rao and K. Motzfeldt, Acta Chemica Scandinavica, 24 (1970), 2796-2802.
[5] J. Drowart, G. DeMaria, R. P. Burns and M. G. Inghram, J. Chem. Phys., 32 (1960), 1366-1372.
[6] G. De Maria, J. Drowart and M. G. Inghram, J. Chem. Phys., 30 (1959), 318-319.
[7] E. Copland, Z. Metallkd. (2005).
[8] T. Markus and K. Hilpert, *Thermodynamic Investigation of the Vaporization of Solid Poly Crystalline Alumina with Knudsen Effusion Mass Spectrometry*, in E. Opila, J. Fergus, T. Maruyama, J. Mizusaki, T. Narita, D. Shifler and E. Wuchina, eds., *High Temperature Corrosion and Materials Chemistry, V*, The Electrochemical Society, Hawaii, 2004.
[9] M. Heyrman and C. Chatillon, J. Phys. Chem. Solids, In Press, Corrected Proof (2005).
[10] E. Copland, *Measuring the Thermodynamics of the Alloy/Scale Interface*, in E. Opila, J. Fergus, T. Maruyama, J. Mizusaki, T. Narita, D. Shifler and E. Wuchina, eds., *High Temperature Corrosion and Materials Chemistry, V*, The Electrochemical Society, 2004.

[11] L. V. Gurvich, I. V. Veyts and C. B. Alcock, *Thermodynamic Properties of Individual Substances; English Version*, Begell House, 1996.
[12] M. W. Chase, *NIST-JANAF Thermochemical Tables*, American Chemical Society, 1998.
[13] *CODATA Key Values for Thermodynamics*, Hemisphere Publishing Corp, Washington, 1988.
[14] E. Copland and N. Jacobson, *NASA Report, in preparation...*, 2005.
[15] H. A. Wriedt, Bull. Alloy Phase Diagrams 6[6] (1985) 548-553; 567-568.
[16] M. Rother and H. Holleck, J. Chim. Phys.Phys.-Chim. Biol., 90 (1993), 333.
[17] S. Lakiza and L. Lapato, J. Am. Ceram. Soc., 80 (1997), 893-902.
[18] O. Fabrichnaya and F. Aldinger, Z. Metallkd., 95 (2004), 27-39.
[19] G. M. Rosenblatt, *Chapter 3: Evaporation from Solids*, in N. B. Hannay, ed., *Treaties on Solid State Chemistry*, Plenum Press, New York, 1976, pp. 165-240.
[20] M. Inghram and J. Drowart, *Mass Spectrometry Applied to High Temperature Chemistry, High Temperature Technology*, Stanford Research Institute, California, 1959, pp. 338-378.
[21] C. Chatillon, C. Senillou, M. Allibert and A. Pattoret, Rev. Sci. Instrum., 47 (1976), 334-340.
[22] P. Morland, C. Chatillon and P. Rocabois, High Temperature and Materials Science, 37 (1997), 167-187.
[23] C. Chatillon, L. Malheiros, P. Rocabois and M. Jeymond, High Temperature High Pressures, 34 (2002), 213-233.
[24] R. Voorhoeve, *Chapter 4: Molecular Beam Deposition of Solids on Surfaces: ultrathin films*, in N. B. Hannay, ed., *Treaties on Solid State Chemistry*, Plenum Press, New York, 1976, pp. 241-342.

Figure Captions

Figure 1. Al_2O_3 effusion-cells: internal cell-body dimensions 10 mm diameter by 8.6 mm tall, orifice dimensions 1.0 mm diameter by 3.5 mm long. The orifice is offset by 2 mm from cell centerline while the hole in the bottom is part of blackbody source (2.5 mm in diameter by 13.5mm long) used for temperature measurement.

Figure 2. Schematic cross section of vapor source furnace with the insert showing detail of the areas where Al_2O_3 condensation was observed. 1) effusion-cell; 2) Mo envelop for 3 effusion-cells; 3) W-foil (25μm thick) heating element; 4) Ta heat shields; 5) blackbody source; 6) Ta light shield; 7) Mo heat shield support; 8) additional Hf-foil (~150μm thick) "oxygen getter".

Figure 3. SEM image of Al_2O_3 condensation and growth observed on the outer edge of the effusion orifice after 8 hours at 1550±3K.

Figure 4. Measured ion-intensities of Au^+ verses time at 1550±3K.

Figure 5. Measured ion intensities of Al^+, Al_2O^+ and $F = p(Al_2O)/p(Al)$ verses time at 1550±3 K as the orifice closed due to Al_2O_3 condensation.

FIGURES

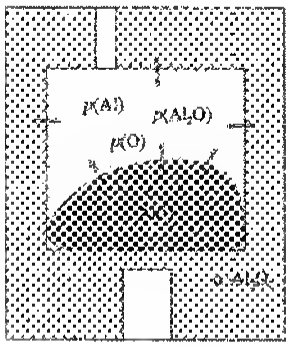

Figure 1. Al_2O_3 effusion-cells: internal cell-body dimensions 10 mm diameter by 8.6 mm tall, orifice dimensions 1.0 mm diameter by 3.5 mm long. The orifice is offset by 2 mm from cell centerline while the hole in the bottom is part of blackbody source (2.5 mm in diameter by 13.5mm long) used for temperature measurement.

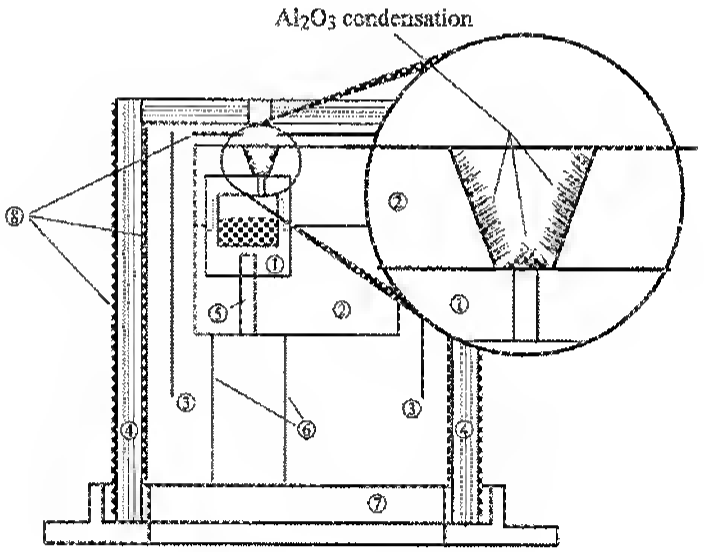

Figure 2. Schematic cross section of vapor source furnace with the insert showing detail of the areas where Al_2O_3 condensation was observed. 1) effusion-cell; 2) Mo envelop for 3 effusion-cells; 3) W-foil (25μm thick) heating element; 4) Ta heat shields; 5) blackbody source; 6) Ta light shield; 7) Mo heat shield support; 8) additional Hf-foil (~150μm thick) "oxygen getter".

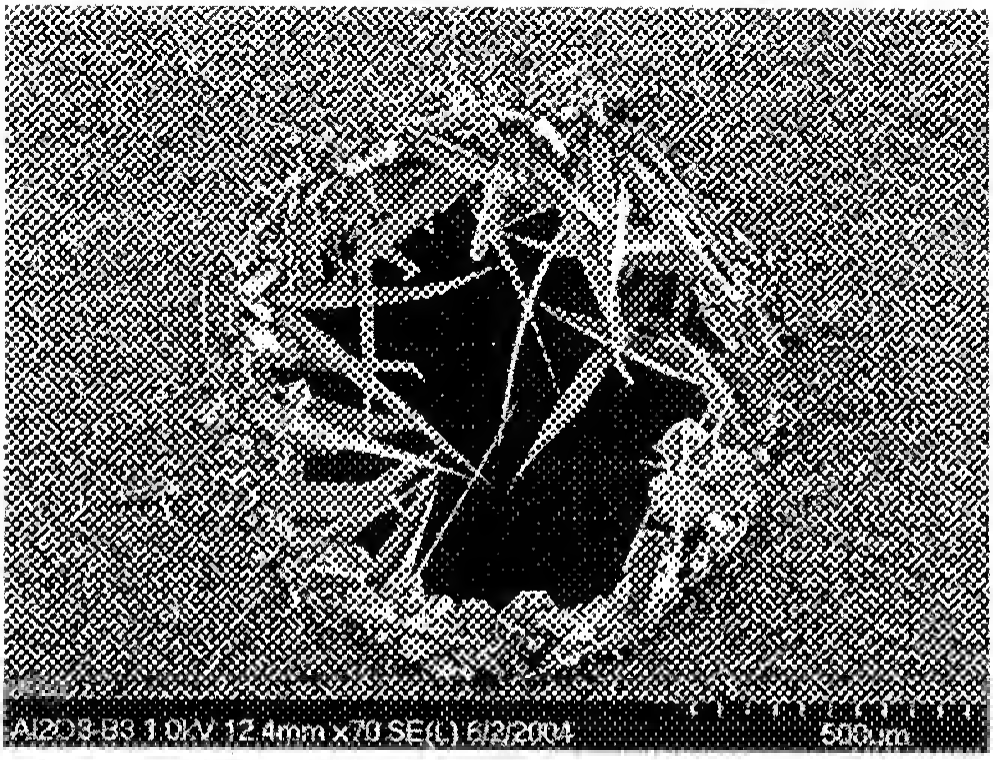

Figure 3. SEM image of Al_2O_3 condensation and growth observed on the outer edge of the effusion orifice after 8 hours at 1550±3K.

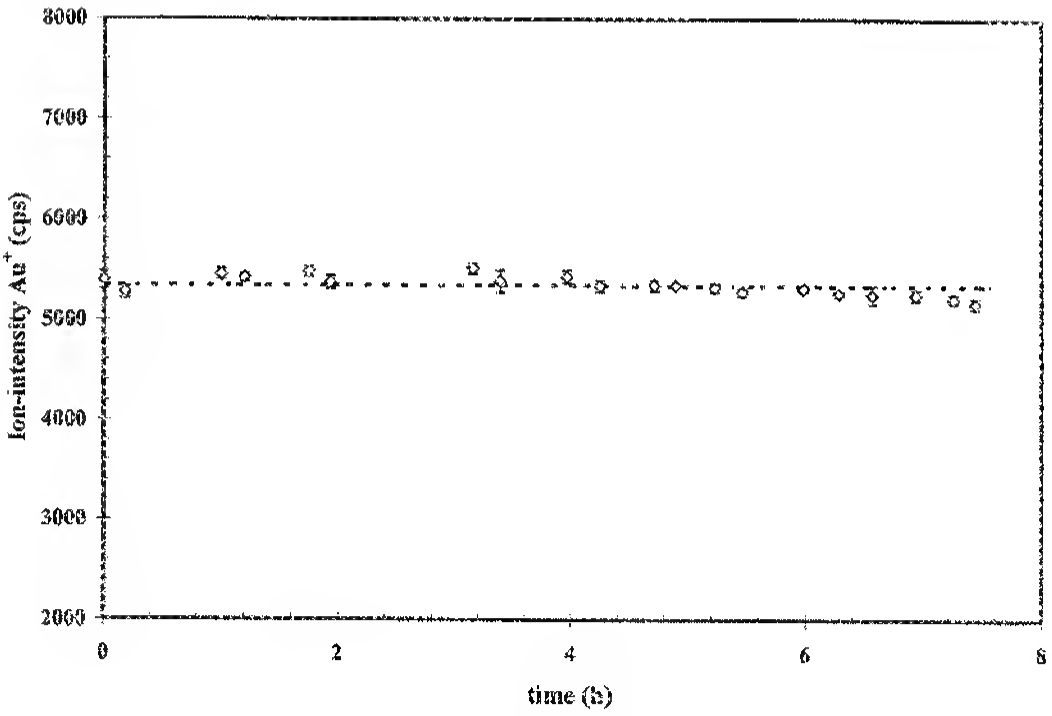

Figure 4. Measured ion-intensities of Au^+ verses time at 1550±3K.

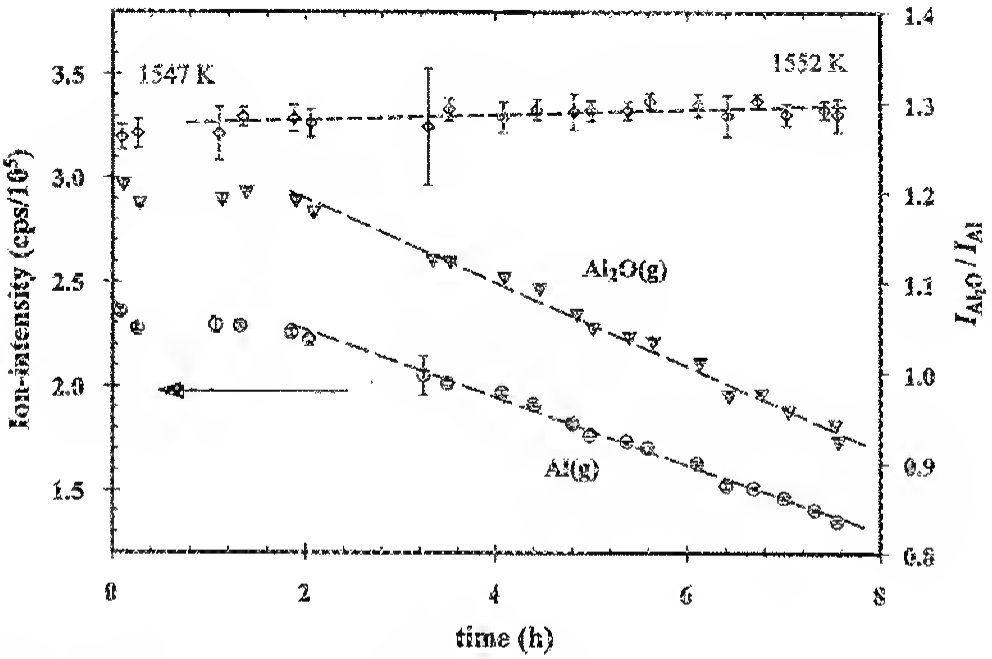

Figure 5. Measured ion intensities of Al^+, Al_2O^+ and $F = p(Al_2O)/p(Al) \propto I(Al_2O^+)/I(Al^+)$ verses time at 1550±3K as the orifice closed due to Al_2O_3 condensation.